Modelling and seismic response analysis of non-residential single-storey existing precast buildings in Italy

Marco Bosio[1], Chiara Di Salvatore[2], Davide Bellotti[3], Luca Capacci[4], Andrea Belleri[1*], Valeria Piccolo[2], Francesco Cavalieri[3], Bruno Dal Lago[5], Paolo Riva[1], Gennaro Magliulo[6], Roberto Nascimbene[7], Fabio Biondini[4]

[1] Department of Engineering and Applied Sciences, University of Bergamo, Bergamo, Italy

[2] Department of Science and Technology, University of Naples Parthenope, Italy

[3] European Centre for Training and Research in Earthquake Engineering, Pavia, Italy

[4] Department of Civil and Environmental Engineering, Politecnico di Milano, Milan, Italy

[5] Department of Theoretical and Applied Sciences, University of Insubria, Varese, Italy

[6] Department of Structures for Engineering and Architecture, University of Naples Federico II, Naples, Italy

[7] University School for Advanced Studies (IUSS), Pavia, Italy

Abstract

Old precast buildings are often characterized by poor detailing that may hamper the structural performance particularly in the case of earthquakes. This is essentially related to: (i) a limited past knowledge of seismic design and behaviour, also reflected in past building codes; (ii) the evolution of seismic zonation of the Italian territory. The aim of this work is assessing the probabilistic seismic vulnerability with respect to the usability preventing damage and global collapse performance levels of four existing single-story precast buildings designed in accordance with past Italian building codes from 1960s to 1990s in three sites with increasing seismic hazard.

1. Introduction

Since its birth, the precast sector has found an important development especially for buildings in the industrial sector. Through precasting, it is possible to execute a whole series of operations within the protected environment of a factory with all the advantages that come with it, both from an economic and technical point of view: better quality control of materials and structural details, speed-up of the erection time, reduction of construction costs, among others. A further advantage of precasting is the possibility to build relatively simple structures able to cover wide spans, enhanced by the use of

---

[1*] corresponding author: andrea.belleri@unibg.it

prestressing technologies, which is a characteristic particularly suitable in the industrial sector, where the flexibility in the management of internal spaces is an important architectural feature in the conceptual structural design.

These systems are typically built as single-story buildings relying on columns' cantilever action to sustain horizontal loading, such as wind and earthquake actions. In general, the columns are installed into socket foundations subsequently filled with concrete or high-strength grout (Osanai et al. 1996) or, more recently, fixed at the foundation base through grouted sleeves or mechanical connections (Dal Lago et al., 2016; Metelli et al., 2011; Belleri and Riva, 2012). The columns are conceived as pin-connected to the main beams (Biondini et al. 2010, Clementi at al., 2016; Magliulo et al., 2014; Zoubek et al., 2014, 2015; Kremmyda et al., 2014, 2017; Rodrigues et al., 2021) and the roof elements are similarly conceived as pin-connected to the supporting beam (Dal Lago and Ferrara, 2018; Dal Lago et al. 2019). The horizontal load transfer between these elements is generally provided by mechanical connection devices, mostly in the form of dowels. However, for wide areas of the Italian territory not yet classified with potential seismic hazard, these joints were created in the past with the simple interposition of elastomeric or metallic pads in between the elements. This type of joint, relying uniquely on the uncertain friction mechanism to transfer horizontal loads, is a source of strong vulnerability.

Up to the 1980s, the most common solution for lateral cladding was relying on infill walls made by masonry or precast panels, while, in modern buildings, the lateral cladding is generally provided by external precast panels attached to the main structural elements. Limited attention was paid up to recently to the cladding-structure interaction (Biondini et al., 2013; Belleri et al., 2016, 2017; Scotta et al., 2015; Zoubek et al., 2016) due to the non-structural conception of the claddings, which yields another potential source of strong vulnerability.

The major seismic vulnerabilities in precast industrial buildings were highlighted during past earthquakes and well documented in the literature (Belleri et al., 2015a; Belleri et al., 2015b; Casotto et al., 2015; Ercolino et al., 2016; Bournas et al., 2014; Magliulo et al., 2014; Minghini et al., 2016; Nastri et al., 2017; Palanci et al., 2017; Savoia et al., 2012; Toniolo and Colombo, 2012; Biondini and Toniolo, 2009). Typical observed collapses were related to the loss of support of roofing elements and/or beams, overturning of cladding panels, and failures at the beam-column joint, such as dowel failure or RC forks out-of-plane failure (Brunesi et al., 2015; Belleri et al., 2016; Belleri et al., 2017; Scotta et al., 2015; Colombo et al. 2016; Demartino et al. 2018; Torquati et al., 2018; Ercolino et al., 2018; Bosio et al. al., 2020; Sousa et al., 2020b).

The work described in this article is part of a larger research project having the task of assessing the seismic vulnerability of existing Italian structural typologies (i.e., RINTC-E, Iervolino et al. 2021) as

a function of different construction periods, and therefore different building codes prescriptions. Previous work was devoted to evaluate the failure rates for Italian buildings designed following modern anti-seismic regulations (Iervolino et al., 2018), therefore estimating the implicit risk of code-conforming buildings. At this regard, specific works on precast RC structures can be found in Magliulo et al. (2018, 2021), Gajera et al. (2021), and Bressanelli et al. (2021).

This paper addresses the seismic performance of four different existing precast industrial buildings designed in accordance with past Italian building codes and located in three sites with increasing seismic hazard: Milano, Napoli, and L'Aquila. The original drawings and detailing are directly taken as reference for the buildings located in Milano (not addressed as a seismic site for the considered building codes), while a simulated re-design following past building codes is carried out for the other two sites, in the case the past regulations classified the considered site as seismic prone. Multi-stripe analyses is performed by non-linear dynamic analyses at ten intensity levels accounting for record-to-record variability. Two performance levels are identified, namely the Usability Preventing Damage (UPD) and the Global Collapse (GC). The results allow to compare the influence of various structural arrangements and detailing on the seismic vulnerability of existing precast industrial buildings typical of the Italian territory during some reference decades.

2. Past Italian building codes for precast concrete structures

Since the analysed buildings are dated back to different construction periods (ranging from 1960s to 1990s), a brief overview on the seismic codes employed in Italy in these decades is given further.

For all the considered past regulations, buildings are regarded as an ensemble of parallel frames; for this reason, the seismic calculation is not performed on the three-dimensional structural model, but only on the most representative frame for each of the two principal directions. Accordingly, once the horizontal seismic force is computed, it is applied independently along both the horizontal orthogonal directions of the structure. Regarding vertical seismic loads, their contribution could be generally neglected for ordinary buildings, although some exceptions apply, as for instance in the case of buildings with beams having a span greater than 20m and in the case of cantilever beams.

In accordance with the reference building code for seismic regions in the 1980s and 1990s (Technical standards for constructions in seismic areas, DM 108, 1986), the Italian territory was subdivided into four different seismic categories. According to such code, the considered sites, i.e., Milano, Napoli, and L'Aquila, are classified as non-seismic (4th category), 3rd seismic category and 2nd seismic category, respectively. The so called "degree of seismicity" (S) is assigned for each category: as reported in Table 1, S is equal to 9 and 6 for the 2nd and 3rd seismic category, respectively. In addition, the building code introduces two other parameters: the response coefficient $R \leq 1$ with the aim of

reducing the seismic load for building periods greater than 0.8s ($R = 1$ if the building period is not computed) and an importance factor I, ranging from 1 to 1.4, to consider the building category of use. Once such coefficients have been defined, it is possible to evaluate the total horizontal (F_h) and vertical (F_v) seismic load for the building:

$$F_h = R \cdot C \cdot I \cdot W \tag{1}$$

$$F_v = m \cdot C \cdot I \cdot W \tag{2}$$

where W is the building total weight, m is an amplification coefficient, typically set equal to 2, and $C = \frac{S-2}{100}$ depends on the seismic intensity. It is worth noting that the amplification coefficient for the vertical design load is strictly defined as at least twice the amplification coefficient for the horizontal action. Another reference document for precast structures in those years is "Prefabrication and precast structures" (CNR 10025, 1984), provided by the Italian National Research Council (CNR). Relevant aspects of the document are related to the structural concept and the connections between elements: "for the purposes of the stability of the buildings, if the functional capacity of the frame is not proven, the stability must be provided by suitable structures able to function as bracing and able to carry the whole horizontal actions. [...] For industrial buildings, joints by simple friction between the secondary roof frame and the main beams are not recommended unless appropriate measures are provided to prevent non-reversible sliding on the contact surfaces". Considering the RC forks at the top of the columns, a minimum thickness of 9 cm in the bottom part of the fork and 7 cm in the upper part is suggested. For simply supported long span girders, the designer should account for the beam stability under various conditions, such as geometry imperfections due to construction or erection and impact or wind loading conditions.

Specific comments apply to precast panels and connecting devices are required to anchor the panel to the supporting elements: the columns, in the case of panels spanning horizontally, the footing and the top beam, in the case of panels spanning vertically. Such connections must be mechanical, readily working and not accounting for friction due to gravity. The anchoring on the support element must be placed in the resistant concrete core at a distance greater than 4cm from the edge of the element and 2cm from the reinforcing bar. Finally, for non-load-bearing panels it is useful to remember that the connections must be such as not to affect the structural stiffness and they should provide a ductile behaviour.

The reference building code in the 1970s is DM 30.05.74 (Technical standards for RC constructions and precast RC constructions in seismic areas). The seismic classification is reported in the Ministerial Decree of 3 March 1975 based on DM 629, stating that Napoli and Milano are not seismic prone areas, whereas L'Aquila falls in 2nd seismic category. The equations to evaluate the total

1 horizontal (F_h) and vertical (F_v) seismic load for the building are similar to the ones given in the 1980s

2 codes:

$$F_h = k_h * W \qquad\qquad (3)$$

$$F_v = k_v * W \qquad\qquad (4)$$

3 where the seismic horizontal coefficient is equal to $k_h = C * R * \varepsilon * \beta * \gamma$; ε is the foundation

4 coefficient, generally assumed equal to 1, except for compressible soils; β is the structure coefficient

5 assumed equal to 1 for frame structures; γ is the coefficient of distribution of the seismic actions,

6 equal to 1 in single-story buildings; C is defined as previously addressed. The seismic weight W is

7 the sum of the self-weight and the accidental loads amplified by a coefficient s, which, for industrial

8 buildings, is equal to 0.33. The seismic vertical coefficient k_v is equal to 0.2.

9 The reference Italian building code in the 1960s is constituted by the Royal Decree of 1939 (Regio

10 Decreto 2229/39) and the document "CCLL Circolare No. 1472/1957". For the seismic classification,

11 the reference legislation is represented by Law no. 1684 of 25 November 1962 "Building measures,

12 with particular prescriptions for seismic areas", according to which L'Aquila belonged to the 2nd

13 seismic category, while Napoli and Milano were not classified as seismic. Seismic provisions in the

14 1960s were the same in the 1970s.

15 *Table 1. Seismic classification of the Italian sites under consideration*

Site	1960s and 1970s	1980s and 1990s
Milano	Not classified	Not classified
Napoli	Not classified	3rd cat. (S=6)
L'Aquila	2nd cat. (S=9)	2nd cat. (S=9)

16

17 **3. Considered case studies and modelling assumptions**

18 **3.1 Case studies**

19 The first structural system (*EE1*) refers to a single-storey precast structure built in 1972 and designed

20 based on static analysis (Figure 1). The geometry of the investigated structure was regularized,

21 analysing a single 20m span of the original building: this structural configuration substantially

22 corresponds to the lateral span of the real building with total plan size 20x54m^2. The columns are

23 precast elements with 0.35x0.35m^2 cross-section and 6m height. The main beams in the transverse

24 (Y) direction have a span of 20m and a double slope (10% inclination) with an I-section variable in

25 both height and thickness. The secondary beams in the longitudinal (X) direction are 6m long with

26 an inverted double-tee cross-section. The assumption of rigid diaphragm was adopted for the roof,

27 given the presence of cast-in-place concrete topping with continuous steel reinforcement between the

28 inverted double-tee roof elements. For such reason, the connection between the roof element and the

29 supporting beam is considered fixed in the analyses. The masonry infill panels, 4.5m high, do not

1 cover the total column height, creating a ribbon window; such infill elements were assumed to be

2 present on all sides of the building.

3 Four site cases were considered. The original resized structure was investigated for soil type C for

4 Napoli and Milano, which at the time of the design were not classified as seismic sites. For L'Aquila,

5 two simulated designs were carried out in accordance with the 1960s (with smooth reinforcement

6 steel bars) and 1970s codes provisions. Regarding the beam-column connection, a simple frictional

7 connection was adopted for the sites of Napoli and Milano, whilst a dowel connection was introduced

8 for the sites of L'Aquila 1960s and 1970s. The properties of the main construction details in the

9 considered sites are reported in Table 2.

10
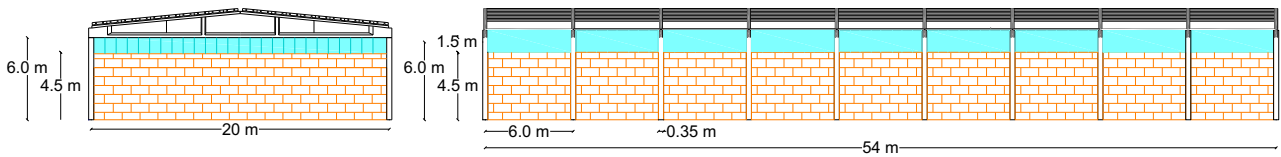
11

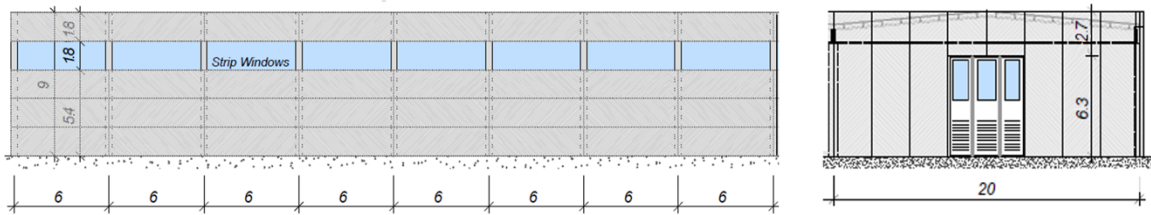12 *Figure 1. Frontal and side view of the EE1 building (Units: m).*

13 *Table 2. Main construction details of EE1 building.*

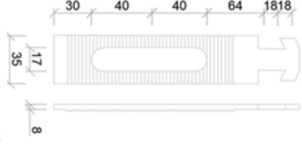|	Milano	Napoli	L'Aquila 1960s	L'Aquila 1970s
Column cross-section	35cm x 35cm	35cm x 35cm	50cm x 50cm	55cm x 55cm
Column longitudinal rebars	4 ϕ18	4 ϕ18	12 ϕ16	8 ϕ18
Column stirrups	ϕ6 at 25cm c.c.	ϕ6 at 25cm c.c.	ϕ8 at 25cm c.c.	ϕ8 at 25cm c.c.
Beam-column connection	Friction	Friction	Dowel	Dowel
Roof-element-beam connection	Fixed	Fixed	Fixed	Fixed
Cladding system	Masonry infills	Masonry infills	Masonry infills	Masonry infills

14

15 The case study referred to the 1980s (*EE2*) is inspired by a building characterized by a plan dimension

16 of 20x42m^2 with eight bays of 20m span spaced at 6m of axis-to-axis distance (Figure 2). Along the

17 longitudinal (X) direction, the closure towards the outside is made by three layers of precast RC

18 horizontal cladding panels connected to adjacent columns, a ribbon glazing system, and an additional

19 layer of cladding panels. Bearing connections are provided at the bottom of every single panel, and

20 out-of-plane restraint connections are provided at the top, with hammer-head bolts anchored in

21 channels embedded within the columns. Along the transverse (Y) direction, precast RC vertical

22 cladding panels spanning from the foundation to the main girder are provided. The panels are

23 anchored to the grade beam at the lower level with a perfectly cylindrical hinge connection and to the

24 main girder at the top by means of a hammer-head stripe connection anchored in steel channels. The

25 main girders are made by prestressed RC double-tapered I-shape beams supporting prestressed RC

26 double-tee precast elements. Gutter beams are provided along the longitudinal sides of the building.

As previously mentioned, the design of the building is compliant with the codes enforced at the construction time (1980s). For the case of Milano, which was classified as a non-seismic site at the hypothetical time of construction, the design provisions and building characteristics are defined starting from the available documentation and structural details of a companion building in a non-seismic region. Different building code prescriptions are adopted for Napoli and L'Aquila, which were classified as seismic sites. It is worth noting that the column cross-section for L'Aquila site had to be re-designed. It is particularly interesting to observe that for the Milano site the structural details do not foresee any type of mechanical connection between the elements, in accordance with the non-seismic classification of the existing building site. Only the out-of-plane restraint of the main girders was provided by means of RC forks placed at the top of the columns. Regarding the mechanical characteristics of the construction materials, concrete strength and rebars yielding strength are 43MPa and 470MPa, respectively, in accordance with material tests on the reference building. The yield strength of the steel used for the cladding connections and dowel connections is assumed to be 300MPa. The properties of the main construction details in the considered sites are reported in Table 3.

Figure 2. Frontal and side view of the EE2 building (Units: m).

1

Table 3. Main construction details of EE2 building.

	Milano	Napoli	L'Aquila
Column cross-section	50cm x 40cm	50cm x 40cm	50cm x 50cm
Column longitudinal rebars	12 ϕ14	12 ϕ14	14 ϕ14
Column stirrups	ϕ8 at 20cm c.c.	ϕ8 at 20cm c.c.	ϕ8 at 20cm c.c.
Beam-column connection	RC fork 7cm x50cm 6+6 ϕ8	RC fork 10cm x50cm 6+6 ϕ8	RC fork 12cm x50cm 6+6 ϕ8
Roof-element-beam connection	Friction	Dowel connection (ϕ10)	Dowel connection (ϕ10)
Horizontal cladding connection	<u>Top connection:</u> Hammer-head bolt ϕ16 Anchor channel 40x2.5mm <u>Bottom connection:</u> Bearing bolt ϕ24 on steel bracket		
Vertical cladding connection	<u>Top connection:</u> Anchor channel 40x2.5mm hammer-head stripe bolt <u>Bottom connection:</u> perfect cylindrical hinge		

2

3 The further case study referring to the 1970s (*EE3*) is a single-story RC precast building with a plan

4 dimension of 45.4x24.4m^2 designed in 1973 without seismic provisions. A single bay is considered

5 along the transverse (Y) direction and nine bays, 5m span each, are considered in the longitudinal (X)

6 direction. 5 columns are present along the transverse direction at the building sides. The cladding

7 system is made of strong infills with 25cm thick hollow masonry bricks. Beams are placed along both

8 the horizontal directions of the building, namely double-slope truss RC principal beams (Figure 3a)

9 along the Y direction and girder RC secondary beams along the X direction. Each main beam is

10 housed on a wedge at the top of the column, with the interposition of a single-layer neoprene pad

11 (Figure 3b). The secondary beams have a constant U-section and they are connected to the top of the

12 columns with a ϕ14 dowel, with the interposition of a neoprene pad (Figure 3b). The roof is made by

13 prestressed double-tee elements connected through a cast-in-place RC topping. It is worth noting that

14 the main beams are not mechanically connected to the columns and the horizontal loads are

15 transferred by friction. The reference building was considered located in Napoli and Milano (non-

16 seismic sites in the 1970s), whilst a simulated seismic design of the longitudinal reinforcement was

17 performed by the authors for L'Aquila (seismic site). The properties of the main construction details

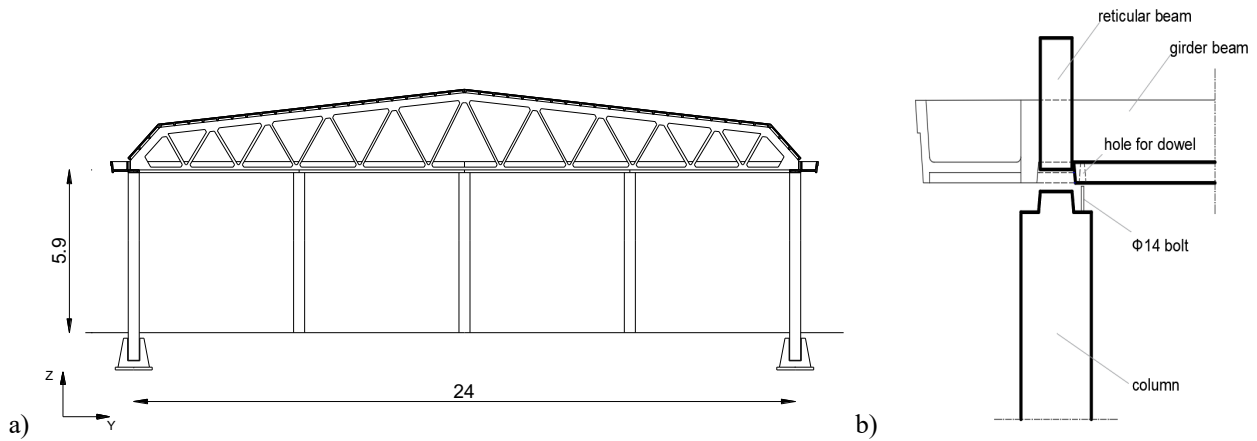18 in the considered sites are reported in Table 4.

19

Figure 3. a) Cross-section of the EE3 building (Units: m). b) beam column connection details.

Table 4. Main construction details of EE3 building.

	Milano	Napoli	L'Aquila
Column cross-section	40cm x 40cm	40cm x 40cm	40cm x 40cm
Longitudinal rebars: main columns	4 ϕ16 + 2 ϕ14	4 ϕ16 + 2 ϕ14	6 ϕ16 + 8 ϕ14
Longitudinal rebars: inner columns in the transverse direction	4 ϕ20 + 4 ϕ22	4 ϕ20 + 4 ϕ22	4 ϕ20 + 4 ϕ22
Column stirrups	ϕ5 at 25cm c.c.	ϕ5 at 25cm c.c.	ϕ5 at 25cm c.c.
Beam-column connection	Friction	Friction	Friction
Cladding system	Masonry infills	Masonry infills	Masonry infills

The case study of the 1990s (*EE4*) is based on an existing industrial building designed and assembled in 1999 in a location falling within the basin hit by the Emilia earthquake sequence in 2012. This building is representative of modern precast industrial buildings, and is characterised by a large structural grid dimension, being the grid modulus 20m by 25m and the clear height of the columns 11m. The extended plan geometry of the original structure has been simplified with an investigated plan dimension of 100m by 75m consisting of five principal bays covered by H-shaped beams along the span of 20m in the longitudinal X direction and three principal bays covered by wing-shaped roof elements (Dal Lago, 2017) along the span of 25m in the transverse Y direction (Figure 4). The primary columns (rectangular cross-section) are fixed at the base with pocket foundations and support the H-shaped beams over a corbel with protruding shear keys in the direction of the floor elements and a double-dowel connection in the direction of the beams. The double-dowel connection acts in both directions to restrain the floor elements to the top of the H-shaped beams. Additional columns having rectangular cross-section unconnected to the main frame structure are placed along the perimeter to support the peripheral horizontal cladding panels. Three rows of rectangular precast sandwich cladding panels are stacked one over the other through a male-female joint; the lowest panel is directly supported over the column foundation footings. A continuous ribbon glazing system is placed above the three rows, and two additional (4th and 5th) rows of cladding panels are present above the ribbon

1   glazing. The 4th row of horizontal panels is supported at the bottom by steel bracket profiles embedded

2   into the columns. The 5th row of horizontal panels transfers the gravity loads directly to the 4th row

3   of panels. Out-of-plane restraints made by double-channel profiles jointed by a steel strap connect

4   each panel to the adjacent columns near the panel corners. For the top cladding panel only, the four

5   profiles are attached in a line to either the top of the beam or roof elements, depending on the building

6   side where they are installed. The reference building was considered in the non-seismic site of Milano,

7   about 150km from the real location of the building within the same large Po valley and identically

8   seismically classified. The frame structure was redesigned for the sites of Napoli and L'Aquila in

9   accordance with the standard in use in the reference period (DM 09/01/96 and DM 14/02/1992).

10 It is worth to note that the lateral load resisting system of the building was practically unaffected by

11 the seismic design, as a consequence of the combination of (i) the high slenderness of the columns,

12 (ii) the use of the allowable stress method, and (iii) the moderate seismic load originated from the use

13 of DM 108/1986 with respect to the design wind load. As a matter of fact, the column cross-section

14 and details were governed by the control of buckling limitation requirements, particularly for

15 locations with a higher snow load such as Milan and L'Aquila. The same number of dowels in the

16 roof and beam connections are obtained in the three sites due to similar horizontal actions associated

17 with wind loads. Moreover, the choice of the producer was to employ strong beam-to-column dowels

18 to avoid overturning failure of the beam elements under erection phases, and therefore their

19 dimensioning is not directly dependent upon the design ordinary loads, including seismic load.

20 Taking as reference a nominal C45/55 concrete class and FeB44k steel grade, a confined concrete

21 compressive strength equal to 53MPa and a rebar steel yielding strength equal to 495MPa are

22 considered in the analyses. The properties of the main construction details in the considered sites are

23 reported in Table 5.

24 a)   b)
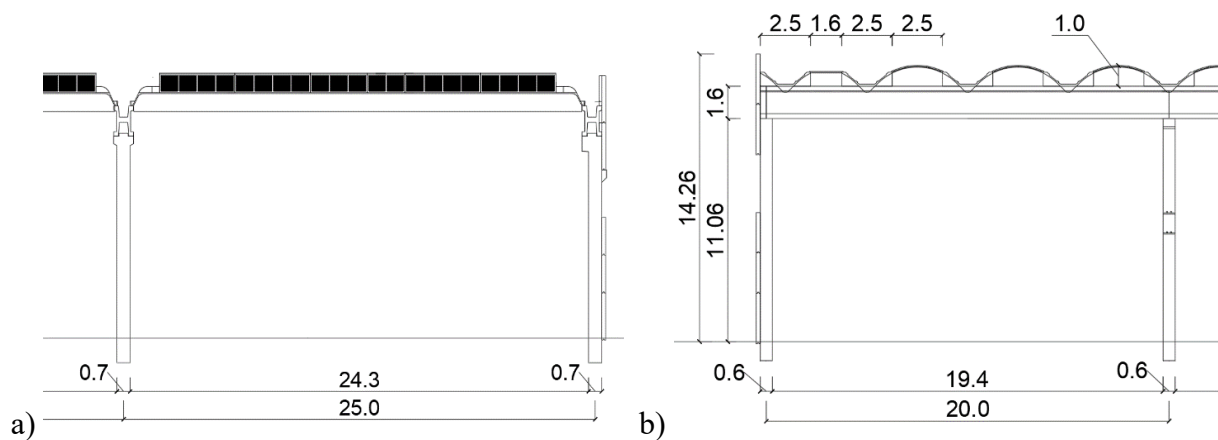
25
26 *Figure 4. Cross-sections of the EE4 building: a) parallel to the wing-shaped roof elements (Transverse direction Y); b) parallel to the H-beams (Longitudinal direction X). (Units: m)*

27

Table 5. Main construction details of EE4 building.

|	Milano	Napoli	L'Aquila
Column cross-section: frame columns	70cm x 60cm	70cm x 60cm	75cm x 65cm
Column cross-section: panel supporting columns	70cm x50cm	70cm x50cm	70cm x50cm
Longitudinal rebars: frame columns	20 ϕ24 + 4 ϕ14	16 ϕ24 + 4 ϕ14	16 ϕ24 + 4 ϕ14
Longitudinal rebars: panel supporting columns	4 ϕ24 + 8 ϕ20 + 2 ϕ14	4 ϕ24 + 8 ϕ20 + 2 ϕ14	4 ϕ24 + 8 ϕ20 + 2 ϕ14
Column stirrups	4 ϕ6 at 20cm c.c.	4 ϕ6 at 20cm c.c.	4 ϕ6 at 20cm c.c.
Beam-column connections	Dowels: 2 M30 8.8 per end	Dowels: 2 M30 8.8 per end	Dowels: 2 M30 8.8 per end
Roof-element-beam connection	Dowels: 2 ϕ14 per end	Dowels: 2 ϕ14 per end	Dowels: 2 ϕ14 per end
Cladding system	External precast sandwich panels	External precast sandwich panels	External precast sandwich panels
Out-of-plane cladding connection	Hammer-head strap inserted into double channel	Hammer-head strap inserted into double channel	Hammer-head strap inserted into double channel
Gravity load bearing cladding connections	4th panel from the bottom: Steel bracket All other panels: simple support with male-female joint to the panel below or to column foundation footings	4th panel from the bottom: Steel bracket All other panels: simple support with male-female joint to the panel below or to column foundation footings	4th panel from the bottom: Steel bracket All other panels: simple support with male-female joint to the panel below or to column foundation footings

3.2 Modelling assumptions

This subsection highlights the main modelling assumptions adopted in the investigated case studies. The columns were modelled similarly for all case studies by providing a fixed connection at the base due to the effective restraint provided by the embedded part of the column inside the socket foundation and the rigid industrial floor. The main and secondary beams, as well as the roof elements, were considered as linear elastic.

A lumped plasticity approach with plastic hinges at the base of the columns and at the base of the ribbon glazing system in the case of strong masonry infills was used to describe the structural nonlinear behaviour of the columns. The column flexural hysteresis was obtained from the following strategy. First, the moment-curvature curve is obtained from a cross-sectional fiber analysis of the column, in which the stress-strain formulation of Mander et al. (1988) was used for both unconfined and confined concrete. The obtained curve is then converted to a bi-linear curve: the initial stiffness is defined by the first yielding of the reinforcement, while the stiffness of the second branch is defined to maintain the same dissipated energy for both the bi-linear and actual response (i.e., respecting the equality of the areas). The plastic hinge model is defined on the basis of the ultimate moment and the

1   yield rotation through four parameters, namely θ_y, θ_{cap}, θ_{pc} and θ_u in terms of rotations (see Figure 5).

2   In the OpenSees program, the plastic hinge was defined using the "Modified Ibarra-Medina-

3   Krawinkler Deterioration Model with Peak-Oriented Hysteretic Response (ModIMKPeakOriented

4   Material)". When possible, the mechanical parameters according to Fardis and Biskinis (2003) for θ_y,

5   Haselton (2006) for θ_{cap} and θ_{pc} and Ibarra (2005) for the definition of the λ degradation parameter

6   were adopted. The ultimate rotation capacity was defined as: $\theta_u = \theta_{cap} + \theta_{pc}$. To describe the behaviour

7   of the plastic hinge of the columns in the presence of smooth bars, the definitions of yield rotation θ_y,

8   θ_{cap} and θ_{pc} according to Verderame and Ricci (2018) were modified on purpose. No residual strength

9   was considered.

10   Double slope beams were modelled with a constant cross-section with the mean value of the variable

11   height and width. Geometrical eccentricities of the structural elements were accounted for by means

12   of rigid elements: the vertical eccentricity between the column and the beam axis was assumed to be

13   half of the mean height of the beam; when present, the secondary beams are connected to the column

14   forks by hinges: horizontal and vertical eccentricities were considered according to Ercolino et al.

15   (2018). Beam-column friction connections were implemented by means of the "Flat Slider bearing"

16   element of OpenSees, which allows the translation in both the principal horizontal directions at the

17   attainment of the friction force computed following the Coulomb model. The friction coefficient was

18   evaluated following Magliulo et al. (2011) for neoprene–concrete friction as a function of the normal

19   stress acting on the sliding surface. For the dowel connections at the beam-column joints and at the

20   roof element-beam joints, the parameters of the force-displacement curve were evaluated in

21   accordance with Bressanelli et al. (2021) and Magliulo et al. (2021) on the basis of the results of

22   experimental tests and analytical formulations (Dei Poli et al., 1992; Kremmyda et al.,2014, 2017;

23   Zoubek et al., 2015; Ferreira and El Debs, 2000; Sousa et al., 2020a). The implementation of the

24   dowel connections in OpenSees was carried out by calibrating the ModIMKPeakOriented.

25
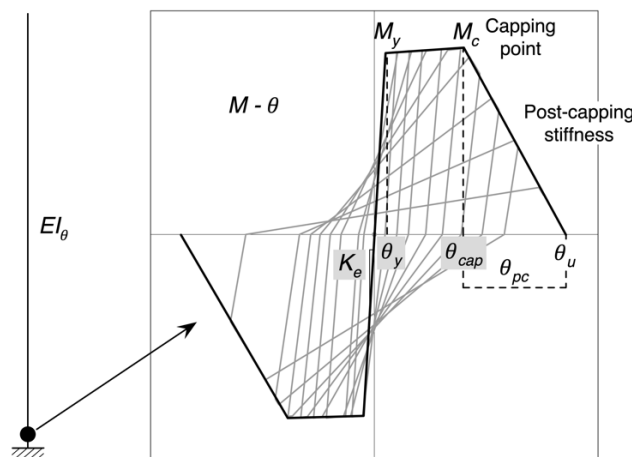
26

27   *Figure 5. Concentrated plasticity approach considered*

1 Regarding the modelling of the RC fork elements (Figure 6), the nonlinearity was associated with the

2 development of a flexural plastic hinge at the fork base by means of the ModIMKPeakOriented

3 material, analogously to the columns. Each RC fork tooth was connected at the base to the head of

4 the column by means of a horizontal rigid element, in order to account for the offset between the axes

5 of the fork tooth and the column; at the top, the RC fork tooth was connected to the main girder by

6 means of a two-node link element with an elastic no-tension material and an additional gap. To

7 capture the possible overturning of the main girder at the RC fork, a stiff element was placed at each

8 side of the girder; this element was connected to each RC fork tooth at its top and to the top of the

9 column at its bottom. An Elastic Multilinear Material was adopted to model the stabilizing moment

10 at the girder support. To account for the variation of the vertical loads, and therefore for the variation

11 of the stabilizing moment, due for instance to the vertical component of the earthquake, a procedure

12 was defined to update the stabilizing moment at each step of the analysis.
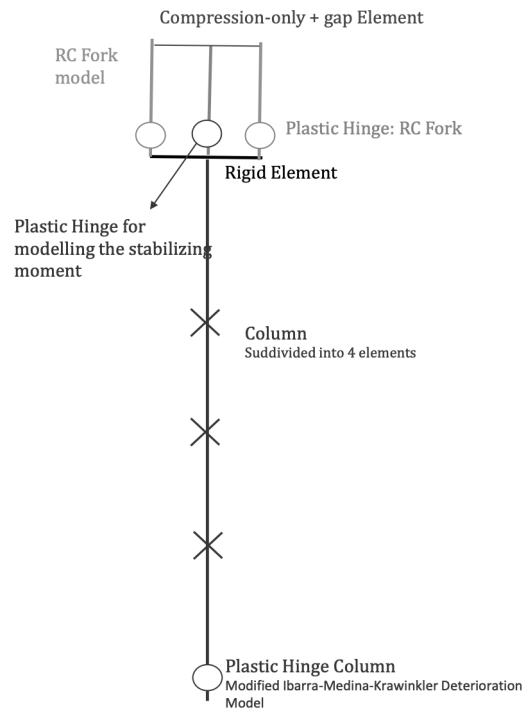
13

14 *Figure 6. Modelling of the RC fork elements.*

15 As for the roof element-beam connections, the actual positioning of the centre of gravity of these

16 elements was considered for the correct assignment of the masses, due to the non-negligible

17 eccentricities given by the position of the roof elements with respect to the beam. Rigid links were

18 introduced (Figure 7) to properly take these aspects into account while preserving both the

19 compatibility of the constraints and the simplicity of the analysis. In the case of mechanical

20 connections at the roof element-beam joint, the connection was assumed made by steel angles bolted

21 between the ribs of the RC double-tee roof elements and the supporting RC beams. Such connections

22 allow the relative rotations of the roof element in its vertical plane while restraining the relative

1 displacements. The nonlinear response of the connection was modelled following the work by Dal

2 Lago et al. (2017) considering hot-rolled steel angles with M16 post-installed mechanical anchors:

3 the response obtained from the researchers during the experimental tests was implemented in

4 OpenSees calibrating the hysteretic behaviour of the MultiLinear nonlinear material.
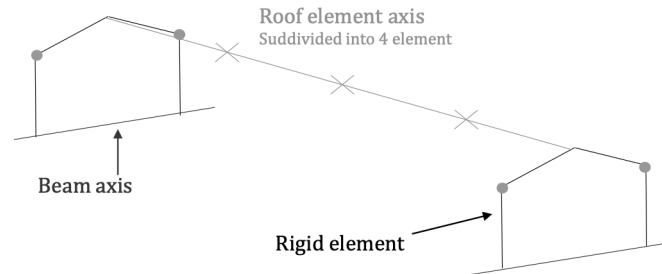
5

6 *Figure 7. Modelling of roof elements.*

7

8 The modelling of the contact between adjacent elements assumes a crucial importance in the model,

9 particularly in the case of friction. Therefore, two-node link elements with an elastic no-tension

10 material were introduced. Such link elements were adopted to connect adjacent roof elements, roof

11 elements to RC curbs placed on top of the girders and roof elements to the gutter beams.

12 For what concerns the masonry infill panels, extended damage was found in older buildings during

13 recent seismic events: the infill panels have often suffered serious damage (important cracks for in-

14 plane mechanisms) or collapsed due to overturning (out-of-plane mechanisms). The most common

15 masonry infill panel found in the Italian precast industrial buildings is constituted by the so called

16 "double-UNI" typology with masonry thickness equal to 0.25m. The infills were modelled following

17 the work of Liberatore et al. (2018), in which different sets of experimental tests available in the

18 literature were used to evaluate the reliability of different models based on the equivalent strut

19 approach. The nonlinear response follows the failure models proposed by Decanini (1986): cracks

20 due to diagonal tension, joint sliding, corner compression and diagonal compression. Regarding the

21 strength of the double-UNI masonry, the following values were considered (Table 6):

22 ● the compressive strength, f_v, of the infill in the vertical direction was assumed according to

23   Colangelo (2005);

24 ● the shear strength of the infill, $\tau_0 = \sqrt{0.285 \cdot f_m}$, was assumed according to Liberatore et al.

25   (2018);

26 ● the shear strength of bed joints, $f_{v0} = \frac{2}{3} \cdot \tau_0$, was assumed according to Liberatore et al (2018);

27 ● the normal modulus of elasticity, E_m, was assumed equal to 2750 MPa ($E_m = 550 \cdot f_m$ derived

28   from FEMA 356).

Table 6. Resistance values of the double-UNI masonry adopted in this study.

f_v	τ_0	f_{v0}	E_{wh}	E_{wv}	G	v
(MPa)	(MPa)	(MPa)	(MPa)	(MPa)	(MPa)	
5.00	0.64	0.43	1200	2750	1400	0.25

The possible reduction of stiffness and ultimate strength of the panel due to the presence of openings was neglected. The modelling strategy adopted involves the use of two diagonal compression-only connecting struts, whose backbone curve was derived from the aforementioned mechanical properties. The strut deformation as a function of the lateral drift was then retrieved on the basis of the expressions proposed by Hak et al. (2012, 2013). The obtained stress and strain values were implemented in OpenSees using the Concrete01 material. In the case of masonry infilled frames with the presence of a ribbon window, an additional lumped plastic hinge was placed at the intersection between the upper end of the equivalent strut and the column in order to model the behaviour of the upper part of the column, failing in flexure.

For the case studies including external cladding panels (EE2 and EE4), the panels were explicitly modelled: beam elements were placed along the axis of the panel to model the panel itself, while rigid elements were placed at each side of the panel to connect the panel axis to the panel-to-structure connections. A distinction needs to be made between top and bottom connections for each panel type. For the top out-of-plane restraining connections there is no significant difference between vertical and horizontal cladding panels, while a different modelling is required for the bottom bearing connections. As regards the top connections, the in-plane behaviour was modelled with a series of "Elastic Perfectly Plastic Gap" materials to capture the sliding of the anchor bolt in the slotted connections (Figure 8) and the stiffness increase due to the contact of the anchor bolt to the end of the slots. An "Elastic Multilinear" material was adopted to model the out-of-plane behaviour of the connections: a high stiffness was assigned to the direction in which the panel comes into contact with the supporting structure, while the actual stiffness associated with the anchor channel lips was assigned to the tear-off direction of the connection. As regards the bottom bearing connections, in the case of horizontal panels the model considered the friction sliding between the panel and the supporting structure and the possible lateral stiffness increase in the case the bearing bolt reaches the end of the seat. For the vertical panels, a cylindrical hinge fixed to the ground was placed at the panel base. Figure 9 depicts a schematic representation of the adopted cladding model.
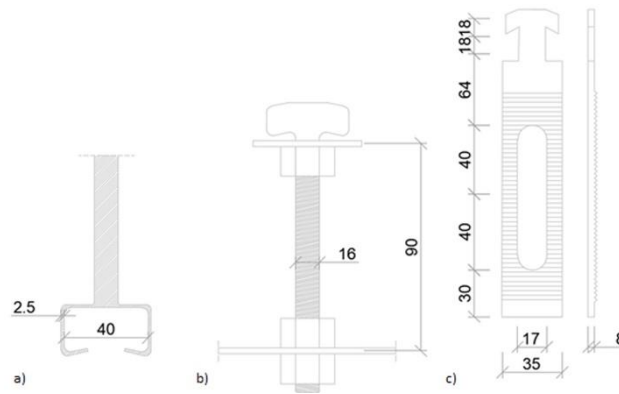
Figure 8. Representation of the anchor bolt used for the cladding panel top connections.
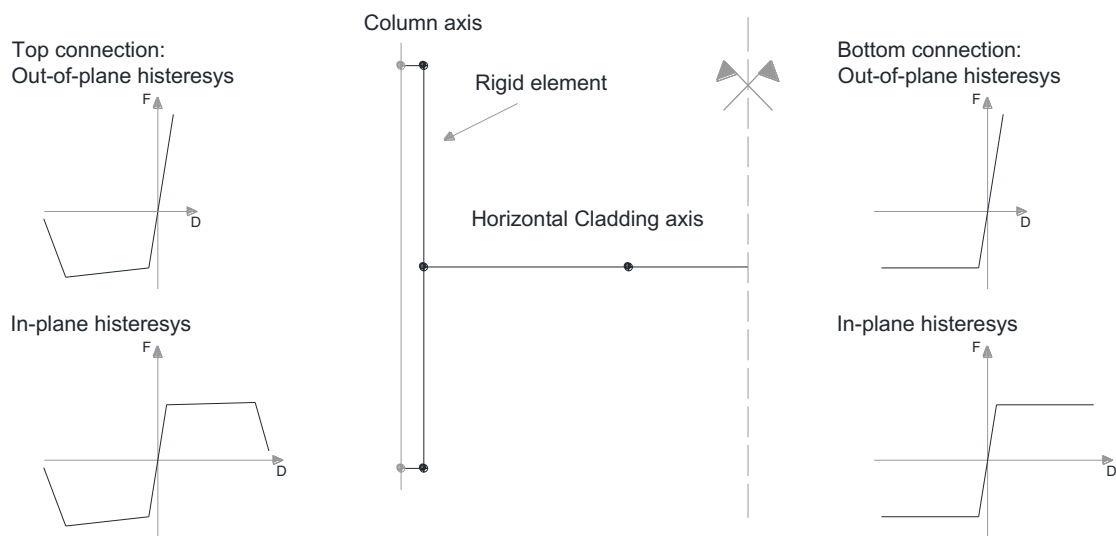*Note: units in mm.*

Figure 9. Schematic representation of the modelling of the cladding at the centre. On the left side the hysteresis of the top connection; on the right side the hysteresis of the bottom connection.

For EE4 building, with horizontal stacked panels, it has been preliminary evaluated that the horizontal limit load on each panel base, calculated after the in-plane failure of the connections, would never bring to the relative sliding of the panels, in the absence of vertical seismic acceleration. Hence, the panel interfaces were modelled as relatively restrained in all translations and rotations but the rotation around the horizontal in-plane axis of the panels, as a result of the presence of male-female joints. The panel above the ribbon glazing system was restrained vertically at its base, and non-linear force-displacement relationships were attributed to the base springs considering both horizontal directions. Such model was calibrated after the experimental tests described in Metelli and Riva (2007). The spring elements modelling the channel-strap connections were provided with specific non-linear force-displacement relationships for in-pane and out-of-plane loading. The in-plane hysteresis was calibrated after the tests carried out by Zoubek et al. (2016), where the model was adjusted to consider the presence of a smaller physical gap (10 mm) between the panel and the frame structure. The out-

of-plane hysteresis was calibrated on the basis of experimental tests described in Menichini et al. 2020. A remove procedure was introduced in the analysis to de-activate a full cladding panel after the failure of a connection device, simulating its full collapse. Despite a similar procedure was introduced to simulate the collapse of the cladding panels stacked above in the case of the failure of a panel below, this option had never been activated during the simulations.

4. Pushover and Multi-stripe analyses

The considered case study buildings were first subjected to nonlinear static (pushover) analyses in both principal directions. Figure 10 shows the results of the pushover analyses for the longitudinal (left side) and transverse (right side) directions. Observing the buildings with masonry infills (i.e., EE1 and EE3), it is evident how the resulting high stiffness leads to the activation of friction for low values of lateral displacements. For EE1 building, the maximum capacity in the longitudinal direction is associated with the development of a flexural hinge in the columns in correspondence to the ribbon glazing system, while in the transverse direction a lower stiffness is observed due to the absence of infill interaction and the lateral capacity is associated with the development of plastic hinges at the base of the columns.

A different behaviour is observed in the two main directions also for EE2 building, with the exception of the Milano site, where the presence of friction connections leads to the sliding of the roof elements at a lower load demand. In that site, a stiffer response is recorded in the longitudinal direction due to a compression-only rigid contact between the roof elements and the RC curb on top of the main beams; such a curb is not present in the case of mechanical connections, such as in the Napoli and L'Aquila cases. In the case of dowel connections at the roof level, a load capacity higher than the Milano case is reached until failure of the connections and subsequent falling of the roof elements in the longitudinal direction, while the transverse direction is governed by the column base flexural capacity. It is worth to note that the presence of cladding panels connected to the main structural elements still provides a global stiffening effect although limited compared to masonry infills. For the transverse direction, the stiffening effects provided by the vertical cladding panels is delayed by the presence of a slotted connection.

On the other hand, analysing in detail the behaviour of EE3 buildings, the pushover curves (Figure 10c) are practically coincident for all the sites, showing a friction-governed behaviour under horizontal loads. Indeed, even if the building was redesigned for L'Aquila site to account specifically for seismic actions, the evaluated horizontal design forces at the joint level (both wind and seismic loads) resulted to be lower than the connection friction resistance, thus making mechanical constraints unnecessary in accordance with the 1970s code provisions. Figure 10c also shows that the pushover curves are characterized by a high elastic stiffness along both the transverse and the longitudinal

direction, due to the presence of infills. Furthermore, it is worth noting that the sliding of the principal beams starts at the same time for all beam-to-column connections due to an in-plane rigid roof diaphragm.

Considering EE4 building, the pushover curves denote a large flexibility associated with the slender column behaviour, characterised by a strong contribution of 2nd order effects. The external horizontal cladding panels and their connection system stiffen the frame structure in the early deformation stage, while such contribution progressively vanishes due to the sequential failure of the connections and the fall of the panels: a sequential in-plane failure of the panels oriented parallelly to the application of the pushover loads occurs around a column drift ratio in the range 0.5% - 2.5%, followed by a sequential out-of-plane failure of the panels oriented orthogonally to the application of the pushover loads induced by the warping generated by the different kinematics of the panel supporting columns and the frame columns, such failure happens for a column drift ratio in the range 2.5% - 3.5%. The response is also dominated by a deformable diaphragm effect, resulting in a larger displacement of the central frames with respect to the outer ones. The building failure is associated with the collapse of the roof-to-beam dowel connections induced by combined inertia loads and indirect actions originated from the diaphragm effect, followed by an immediate loss of support of the roof elements after severe damaging of the joint and concrete spalling.
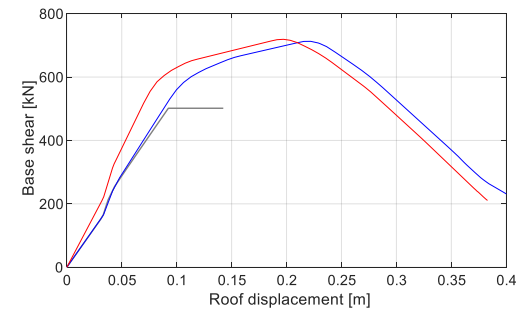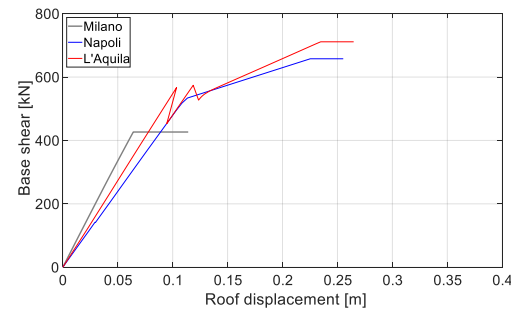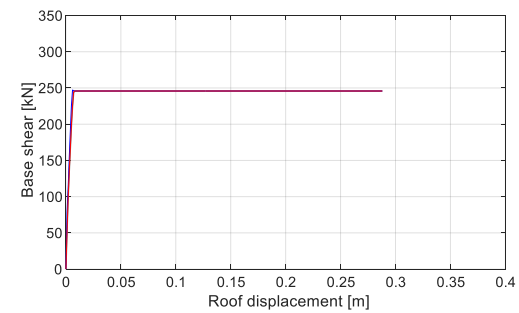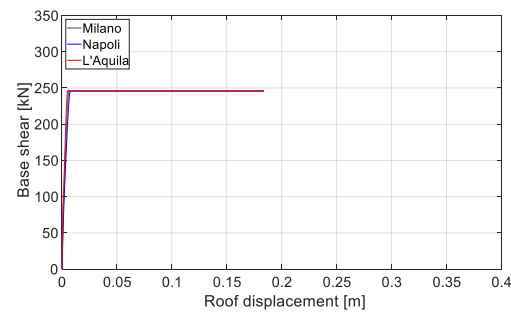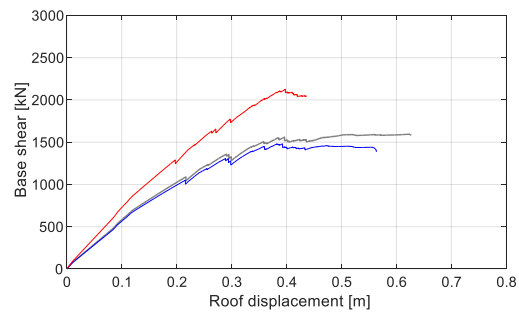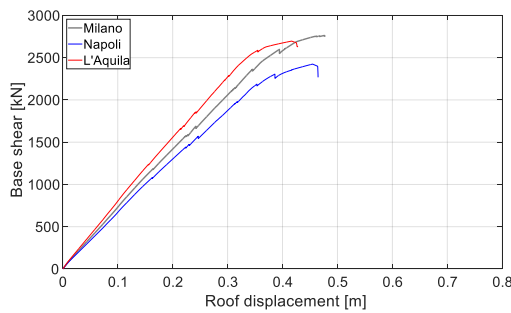
1

a)

2
3

b)

4
5

c)

6
7

d)

8
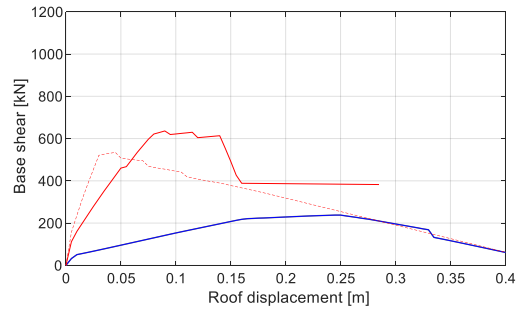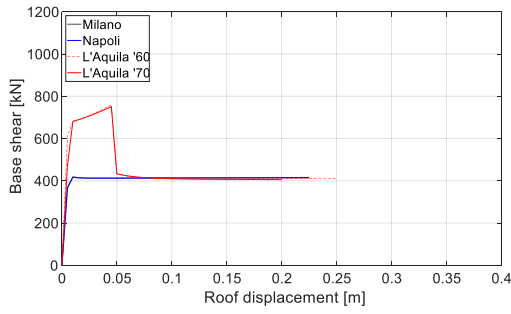
9   *Figure 10. Results of nonlinear static analyses for the EE1 (a), EE2 (b), EE3 (c), and EE4 (d) buildings.*
10   *Note: the left and right side represent the longitudinal (X) and transverse (Y) direction, respectively.*

11

12   The demand-capacity curves resulting from the multi-stripe analyses are reported in Figure 11. The

13   median values of the results of the 20 ground motions for each of the 10 intensity levels were

14   considered and only the envelope curve (i.e. the curve obtained from considering the highest demand-

15   capacity ratio among the various failure mechanisms considered) for each building and for each

16   considered performance level is represented for sake of brevity.

The ground motions and the intensity levels were selected in accordance with the RINTC project (Iervolino et al., 2018, 2021) analogously for the various building typologies considered in the project (i.e., masonry, RC, base isolated, and steel buildings). Ten intensity levels reflecting different earthquake return periods were considered: [10; 50; 100; 250; 500; 1'000; 2'500; 5'000; 10'000;100'000] years.

Figure 11 shows the Usability Preventing Damage (UPD) performance level on the left side and the Global Collapse (GC) performance level on the right side, while each row represents the considered sites: Milano (top), Napoli (middle), and L'Aquila (bottom). Similarly, Figure 12 shows the mean values for the buildings with masonry infills (EE1 and EE3) and with external RC cladding panels (EE2 and EE4). This last figure presents also the results of the previous RINTC-N project regarding industrial precast buildings designed in accordance with modern seismic regulations (Magliulo et al., 2018): only the demand-capacity curve for the L'Aquila site (Bressanelli et al., 2021) is shown, due to the same model characteristics and chosen engineering demand parameter (relative displacement of the beam-column connection); indeed, in the previous project (Magliulo et al., 2018) the beam-column dowel connection was modelled as elastic and the connection failure was determined during post-processing by looking at the connection load instead of at the connection displacement as carried out herein. It is worth mentioning that the case studies of the previous project were characterized by the presence of external cladding panels and by an additional RC topping at the roof level leading a rigid diaphragm behaviour, while herein the considered structural typology could be characterized either by rigid roof diaphragms (EE1 and EE3), in the case of additional RC topping, or flexible roof diaphragms (EE2 and EE4), in the case of precast roof elements directly connected to the supporting beam through dowels or friction.

In this project, the GC failure criteria are related to the achievement of the plastic hinge rotation capacity of the columns (located either at the column base or either at the ribbon glazing system for EE1) and to the loss of support of an element of the roof system, either a precast roof element or a main girder; while, considering UPD, the selected types of damage are: an extensive in-plane damage in the masonry infills, the failure of the connections of precast cladding, a 10% relative displacement in the case of friction connections between the main structural elements, IDR evaluated on the top of the columns reaching 1%. It is interesting to observe how all the considered sites are characterised by a high vulnerability towards this performance level. In particular, it should be noted that for the Milano site, all the buildings saturate the capacity of the related vulnerabilities (sliding of the beam-column friction connections for EE1 and EE3; failure of the cladding panel connections for EE2 and EE4). Analysing the Napoli and L'Aquila sites, similar considerations arise with a UPD capacity reached starting from the 6th and 4th intensity level, respectively. In general, it is observed how the

buildings with external cladding panels (i.e., EE2 and EE4) are characterised by a higher UPD vulnerability compared to buildings with masonry infills (i.e., EE1 and EE3); in particular, in the buildings with infills, the dominant UPD vulnerability is the relative displacement of 10% of the available bearing length in beam-to-column joints, while for building with external precast cladding the dominant UPD vulnerability is the failure of the cladding connections.

As regards GC, the following considerations can be drawn. In the Milano site the maximum demand-capacity ratio is lower than 20% for buildings EE1, EE2 and EE3 (the dominant vulnerability is represented by the deformation demand of the column for EE2 and the sliding of the friction connections for the other cases) and about 50% for EE4 (related to dowel connections). For this low-seismicity site it is interesting to note that the attitude of collapse is limited and the presence of masonry infills and of a roof rigid diaphragm provides a general better performance compared to buildings with external cladding panels, as commonly adopted in the current construction practice.

A higher demand scenario is recorded for the Napoli site, where the EE2 and EE4 buildings saturate the capacity respectively at intensity 10, due to the achievement of the ultimate rotation capacity of the column, and intensity 7 for exceeding the ultimate capacity of the dowel. Also in this site, the buildings with masonry infills are characterised by a lower demand-capacity ratio.

Finally, in the site of L'Aquila it is observed that all the models saturate the capacity of the structure at the intensity, 6, 6, 7 and 5 for the EE1, EE2, EE3, and EE4 building, respectively; while the code-conforming building saturates the capacity at intensity 10. In EE1 the dominant vulnerability is associated with the failure of the dowel connection at the beam-column joint and with the subsequent falling of the beam from its seating; in EE2 the main vulnerability is the column chord rotation up to intensity 5 which is subsequently replaced by the loss of support of the roof elements after failure of the dowel connection; in EE3 the failure is associated with the loss of support of the beam; in EE4 all collapses are related to the failure of roof-to-beam dowel connections.

1
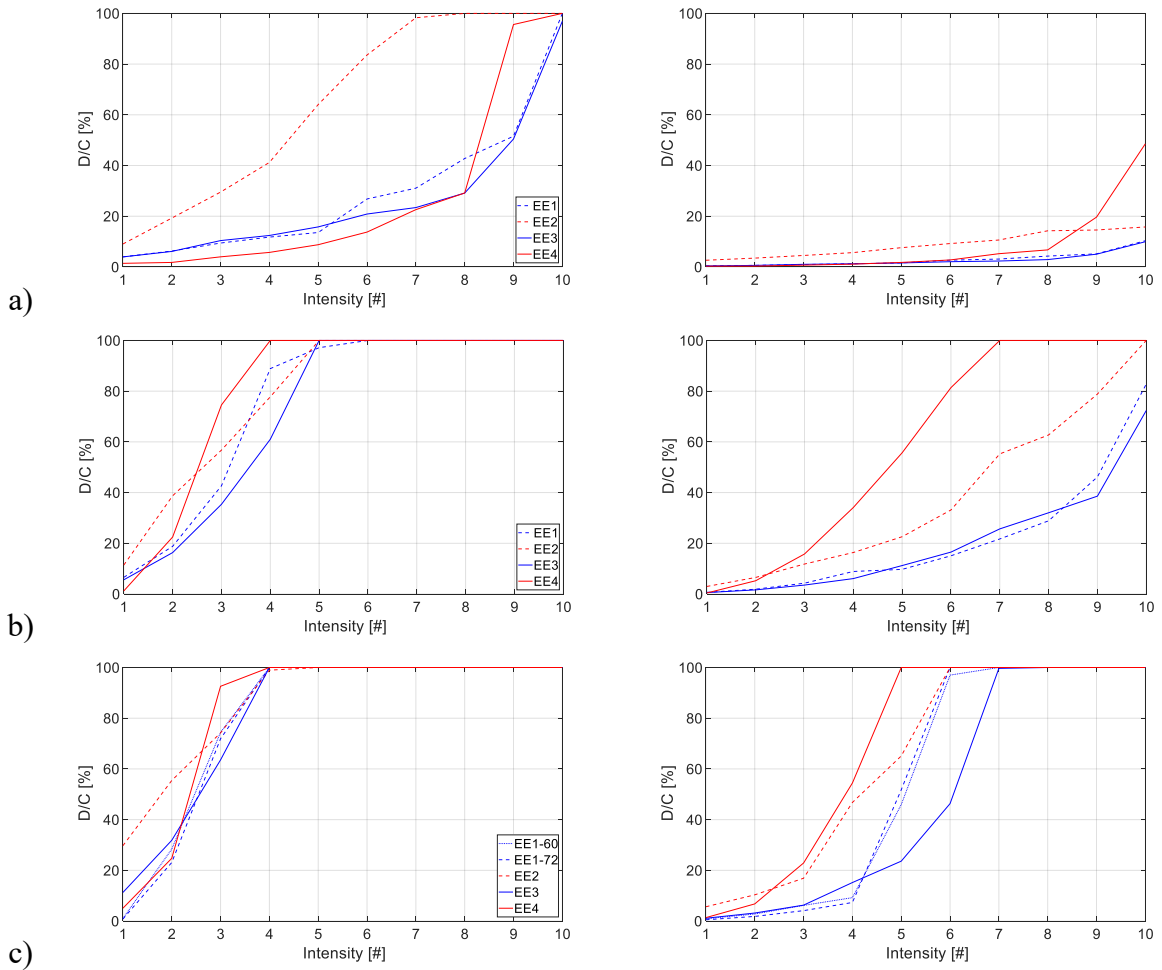

2   a)

3   b)

4   c)
5

Figure 11. Results of multi-stripe analyses in terms of demand-capacity ratio for the sites of Milano (a), Napoli (b), and L'Aquila (c). Note: the left and right side represent the usability preventing damage (UPD) and the global collapse (GC) performance levels, respectively. The intensity levels correspond to the following earthquake return periods: [10; 50; 100; 250; 500; 1'000; 2'500; 5'000; 10'000;100'000] years.

10

1

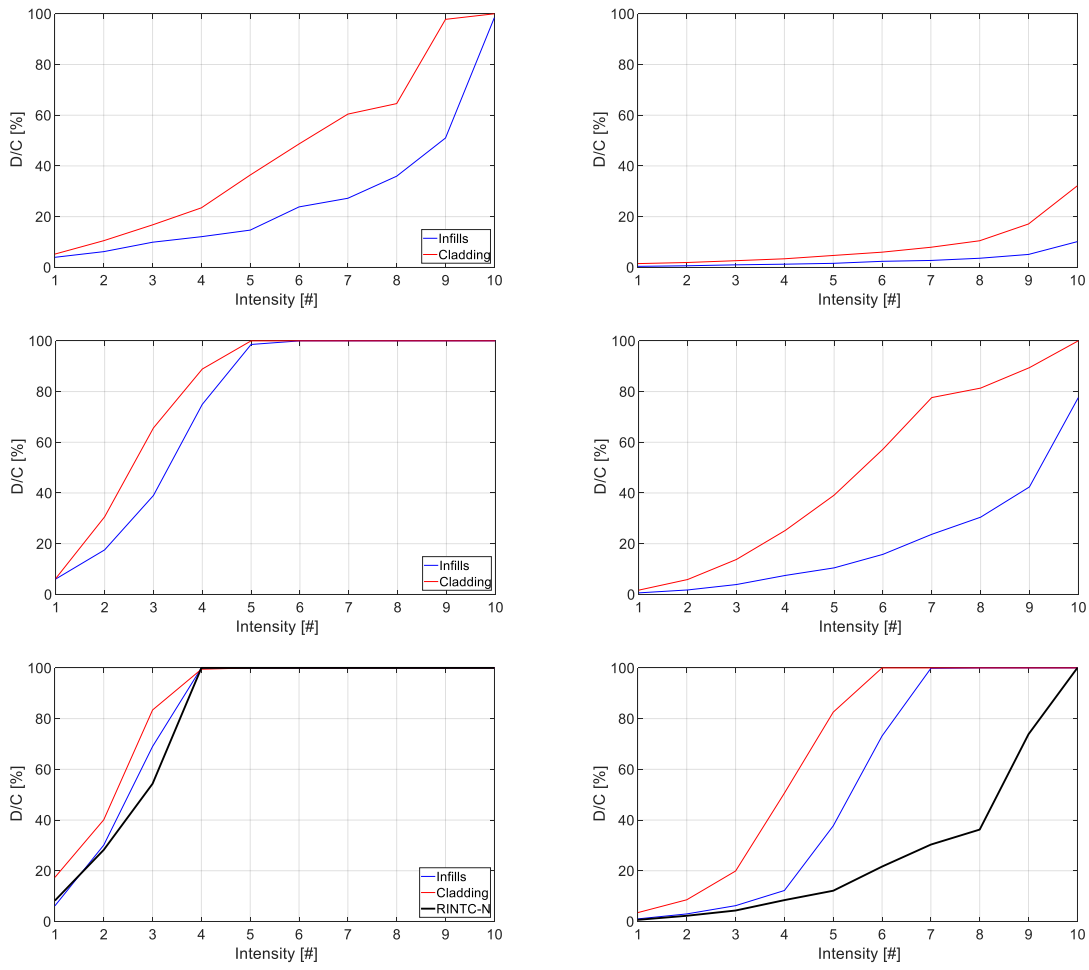2   a)

3   b)

4   c)

5 *Figure 12. Results of multi-stripe analyses in terms of mean values for the buildings with infills (i.e., infills: buildings EE1 and EE3)*
6 *and with external cladding panels (i.e., cladding: buildings EE2 and EE4) in terms of demand-capacity ratio for the sites of Milano*
7 *(a), Napoli (b), and L'Aquila (c). Note: the left and right side represent the usability preventing damage (UPD) and the global*
8 *collapse (GC) performance levels, respectively. The intensity levels correspond to the following earthquake return periods: [10; 50;*
9 *100; 250; 500; 1'000; 2'500; 5'000; 10'000;100'000] years.*

10

11 Finally, Figure 13 shows the results in terms of percentage of analyses per intensity level in which

12 the analysis reaches the capacity associated with UPD and GC. The results consider the mean value

13 of the buildings with infills (EE1 and EE3), the mean value of the buildings with cladding panels

14 (EE2 and EE4), and the mean value of the case studies of the RINTC-N project. The histograms show

15 as expected the higher seismic vulnerability of old buildings compared to code conforming structures

16 for both UPD and GC performance levels. Considering UPD, a general limited difference between

17 old buildings and code conforming structures is observed. It is interesting to note that the old buildings

18 with external cladding panels are the most vulnerable typology for the sites of low and medium

19 seismicity (Milano and Napoli, respectively), with a lower scatter in the medium seismicity site

20 compared to the low seismicity one. The opposite happens for the site of high seismicity (L'Aquila).

Considering GC, only one collapse is observed for the site of low seismicity (Milano). For the site of medium seismicity (Napoli), the buildings with flexible roof diaphragms (EE2 and EE4) are more vulnerable than the buildings with rigid diaphragms (EE1 and EE3). This outcome is also related to considering the falling of a single roof element as "collapse" for the case of flexible diaphragms. For the site of high seismicity (L'Aquila), there is a reduction of the difference of number of collapses between the two types of buildings.

a)

b)

c)
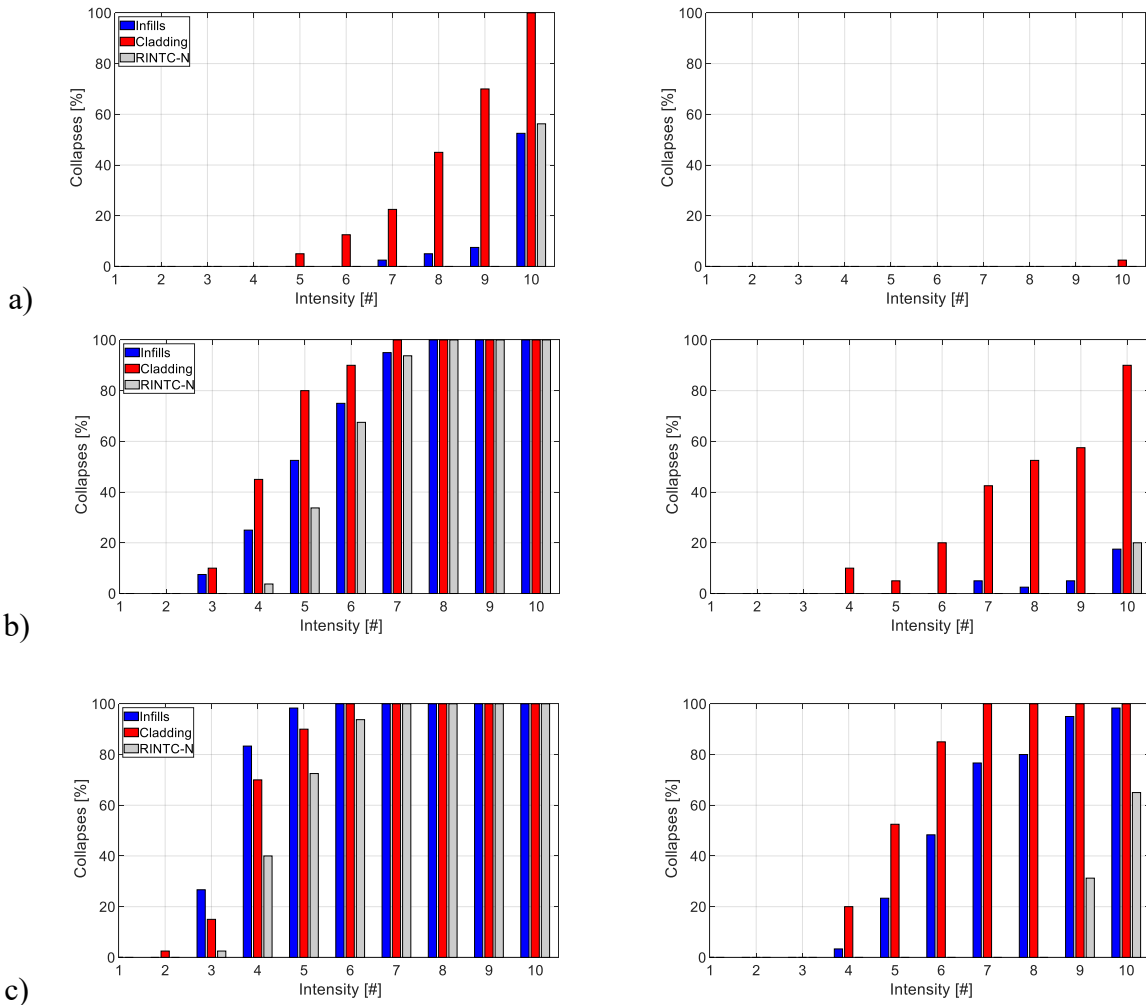
Figure 13. Results in terms of number of "collapses", i.e., in terms of percentage of analyses per intensity level in which the analysis reaches the capacity associated with UPD and GC for the sites of Milano (a), Napoli (b), and L'Aquila (c). Note: the left and right side represent the usability preventing damage (UPD) and the global collapse (GC) performance levels, respectively. The intensity levels correspond to the following earthquake return periods: [10; 50; 100; 250; 500; 1'000; 2'500; 5'000; 10'000;100'000] years.

Conclusions

The present paper investigated the seismic performance of one-storey precast industrial buildings built in accordance with past Italian building codes as part of an Italian national project (RINTC-E) aimed at evaluating the seismic risk of existing buildings with various structural typologies. Herein, four precast buildings have been selected based on different construction periods and typologies: two buildings representative of the decades 1960s and 1970s were characterized by masonry infills on the

building perimeter and by a cast-in-place RC topping at the roof level, which provided an in-plane rigid diaphragm behaviour at the roof level; the other two buildings, representative of the decades 1980s and 1990s, were characterized by external RC cladding panels and by an in-plane flexible roof diaphragm due to the absence of a RC topping. Regarding the connections between structural elements, both mechanical and friction connections have been considered. Three sites in the Italian territory with increasing seismicity have been selected: Milano (low seismic hazard), Napoli (medium seismic hazard), and L'Aquila (high seismic hazard). Each building was designed for each site in accordance with the building code regulation enforced at the time of construction taking as reference existing structural drawings and details for non-seismic sites.

The buildings were subjected to a multi-stripe analysis and the results were presented with respect to two different performance levels: Usability Preventing Damage (UPD) and Global Collapse (GC). UPD was related to failure of connections in the precast cladding panels or to a relative displacement between structural elements greater than 10% of the available bearing length (either after failure of the connections or sliding in the case of friction connections); GC was related to the falling of at least one of the roof elements or to the attainment of the ultimate capacity rotation of at least one plastic hinge in the columns. The results of the analyses have been compared to the results of a previous project (RINTC-N) aiming at evaluating the seismic risk of building typologies built in accordance to current anti-seismic regulations. The results show, as expected, a higher vulnerability of the existing buildings for both UPD and GC performance levels. It is observed that the more modern existing buildings with cladding panels and mechanical connections between precast elements resulted more vulnerable compared to older buildings, which finds an explanation in considering the absence of a rigid diaphragm action in combination with the lack of stiffening contribution arising from peripheral infill panels. The assessment of the relative contribution of these phenomena is a topic of ongoing research. For buildings representative of the decades 1960s and 1970s, the GC is associated with falling of the main roof girders, while, for buildings representative of the decades 1980s and 1990s, the GC is associated with the failure of the roof element connections and subsequent falling of the roof elements. It is worth noting that the difference between the number of collapses of both types of buildings reduces for the site with the highest seismic intensity. Regarding UPD performance level, it is observed that the precast cladding system is more vulnerable particularly for the site with low seismicity, while comparable results are obtained for the sites of medium and high seismicity. For the same sites, similar results are observed in the case of new buildings.

References

Belleri, A., and Riva, P. (2012). Seismic performance and retrofit of precast concrete grouted sleeve connections. PCI Journal 57 (1): 97–109.

Belleri, A., Brunesi, E., Nascimbene, R., Pagani, M., Riva, P. (2015a). Seismic performance of precast industrial facilities following major earthquakes in the Italian territory. Journal of Performance of Constructed Facilities, 29(5). doi: 10.1061/(ASCE)CF.1943-5509.0000617.

Belleri, A., Cornali, F., Passoni, C., Marini, A., Riva, P. (2017). Evaluation of out-of-plane seismic performance of column-to-column precast concrete cladding panels in one-storey industrial buildings. Earthquake Engineering and Structural Dynamics, 47, 397-417. doi: 10.1002/eqe.2956.

Belleri, A., Torquati, M., Marini, A., Riva, P. (2016). Horizontal cladding panels: in-plane seismic performance in precast concrete buildings. Bulletin of Earthquake Engineering, 14, 1103-1129. doi: 10.1007/s10518-015-9861-8.

Belleri, A., Torquati, M., Riva, P., Nascimbene, R. (2015b). Vulnerability assessment and retrofit solutions of precast industrial structures. Earthquakes and Structures, 8(3), 801–820. doi: 10.12989/eas.2015.8.3.801.

Biondini, F., Toniolo, G. (2009). Probabilistic calibration and experimental validation of the seismic design criteria for one-storey concrete frames. Journal of Earthquake Engineering, 13(4), 426-462.

Biondini, F., Toniolo, G., Tsionis, G. (2010), Capacity Design and Seismic Performance of Multi-Story Precast Structures, European Journal of Environmental and Civil Engineering, 14(1), 11-28.

Biondini, F., Dal Lago, B., Toniolo, G. (2013). Role of wall panel connections on the seismic performance of precast structures. Bulletin of Earthquake Engineering, 11(4), 1061-108.

Bosio, M., Belleri, A., Riva, P., Marini, A. (2020). Displacement-Based Simplified Seismic Loss Assessment of Italian Precast Buildings. Journal of Earthquake Engineering 24(sup1). doi: 10.1080/13632469.2020.1724215.

1   Bournas, D.A., Negro, P., Taucer, F.F. (2014). Performance of industrial buildings during the Emilia
2   earthquakes in North-ern Italy and recommendations for their strengthening. Bulletin of Earthquake
3   Engineering, 12(5), 2383–2404. doi: 10.1007/s10518-013-9466-z.

4   Bressanelli ME, Bellotti D, Belleri A, Cavalieri F, Riva P, Nascimbene R. (2021). Influence of
5   Modelling Assumptions on the Seismic Risk of Industrial Precast Concrete Structures. Front. Built
6   Environ. 7:629956. doi: 10.3389/fbuil.2021.629956

7   Brunesi, E., Nascimbene, R., Bolognini, D., Bellotti, D. (2015). Experimental investigation of the
8   cyclic response of rein-forced precast concrete framed structures. PCI Journal 60(2), 57-79. doi:
9   10.15554/pcij.03012015.57.79.

10   Casotto, C., V. Silva, H. Crowley, R. Nascimbene, and R. Pinho. 2015. Seismic fragility of Italian
11   RC   precast   industrial   structures.   Engineering   Structures   94:   122–36.   doi:
12   10.1016/j.engstruct.2015.02.034.

13   CCLL Circolare 23 maggio 1957 n.1472, Armature delle strutture in cemento armato. (in Italian)

14   Clementi, F., Scalbi, A., and Lenci, S. (2016). Seismic performance of precast reinforced concrete
15   buildings with dowel pin connections. J. Building Eng. 7, 224. doi: 10.1016/j.jobe.2016.06.013

16   Colangelo F. (2005). Pseudo-dynamic seismic response of reinforced concrete frames infilled with
17   non-structural brick masonry. Earthquake Engng Struct. Dyn. 34:1219–1241.

18   Colombo A., Negro P., Toniolo G., Lamperti M. (2016). Design guidelines for precast structures with
19   cladding panels, JRC Technical report, ISBN 978-92-79-58534-0

20   Consiglio Nazionale delle Ricerche, CNR 10025:1984: "Istruzioni per il progetto, l'esecuzione ed il
21   controllo delle strutture prefabbricate in conglomerato cementizio e per le strutture costruite con
22   sistemi industrializzati.", 1984. (in Italian)

23   D.M. 30 maggio 1974. Norme tecniche per la esecuzione delle opere in cemento armato normale e
24   precompresso e per le strutture metalliche. (in Italian)

25   Dal Lago B, Toniolo G, Felicetti R, Lamperti Tornaghi M. (2017). End support connection of precast
26   roof elements by bolted steel angles. Structural Concrete, 18, 755–767.

Dal Lago, B. (2017). Experimental and numerical assessment of the service behaviour of an innovative long-span precast roof element. International Journal of Concrete Structures and Materials, 2017, 11(2), 261–273.

Dal Lago, B., and Ferrara, L. (2018). Efficacy of roof-to-beam mechanical connections on the diaphragm behaviour of precast decks with spaced roof elements. Eng. Struct. 176, 681–696. doi: 10.1016/j.engstruct.2018.09.027

Dal Lago, B., Bianchi, S., Biondini, F. (2019). Diaphragm effectiveness of precast concrete structures with cladding panels under seismic action. Bulletin of Earthquake Engineering, 17(1), 473–495.

Dal Lago, B., Toniolo, G., Lamperti Tornaghi, M. (2016). Influence of different mechanical column-foundation connection devices on the seismic behaviour of precast structures. Bulletin of Earthquake Engineering, 14(12), 3485–3508.

Decanini LD, Fantin GE. Modelos simplificados de la mampostería incluidas en porticos. Características de rigidez y resistencia lateral en estado límite. In: Proc of 6th Jornadas Argentinas de Ingenierìa Estructural; 1986. p. 817–36. (in Spanish)

Decreto ministeriale 3 marzo 1975. Approvazione delle norme tecniche per le costruzioni in zone sismiche. (Supplemento ordinario Gazzetta Ufficiale 8 aprile 1975, n.93). (in Italian)

Dei Poli, S., Di Prisco, M., Gambarova, P.G. (1992). Shear response, deformations and subgrade stiffness of a dowel bar embedded in concrete. ACI Struct. J., 89(6):665-675.

Demartino C., Vanzi I., Monti G., Sulpizio C. (2018). Precast industrial buildings in Southern Europe: loss of support at frictional beam-to-column connections under seismic actions. Bulletin of Earthquake Engineering, 16(1):259-294

Ercolino, M., Bellotti, D., Magliulo, G., Nascimbene, R. (2018). Vulnerability analysis of industrial RC precast buildings designed according to modern seismic codes. Engineering Structures, 158, 67-78. doi: 10.1016/j.engstruct.2017.12.005.

Ercolino, M., Magliulo, G., and Manfredi, G. (2016). Failure of a precast RC building due to Emilia-Romagna earthquakes. Engineering Structures, 118, 262-273.

Fardis, M. N. and Biskinis, D. (2003). Deformation capacity of RC members, as controlled by flexure or shear. In Performance-based engineering for earthquake resistant reinforced concrete structures:

a volume honoring Shunsuke Otani, eds. T. Kabeyasawa and H. Shiohara (University of Tokyo, Tokyo, Japan).

Federal Emergency Management Agency. Prestandard and commentary for the seismic rehabilitation of buildings. FEMA 356/November 2000

Ferreira, A., and El Debs, M. (2000). Deformability of beam-column connection with elastomeric cushion and dowel bar to beam axial force. 2nd international symposium on prefabrication.

Gajera K, Dal Lago B, Capacci L, Biondini F. (2021). Multi-stripe seismic assessment of precast industrial buildings with cladding panels. Front. Built Environ. 7:631360. Doi: 10.3389/fbuil.2021.631360

Hak S., Morandi P., Magenes G. (2013). Damage Control of Masonry Infills in Seismic Design, Research Report EUCENTRE No. 01.2013, IUSS Press

Hak S., Morandi P., Magenes G. & Sullivan T. J. (2012). Damage Control for Clay Masonry Infills in the Design of RC Frame Structures, Journal of Earthquake Engineering, 16:sup1, 1-35

Haselton, C. (2006). Assessing seismic collapse safety of modern reinforced concrete moment-frame buildings. P. Report, ed. Department of Civil Engineering California State University, Chico.

Ibarra, L. F., Medina, R. A. and Krawinkler, H. (2005). Hysteretic models that incorporate strength and stiffness deterioration. Earthquake Engineering & Structural Dynamics 34(12), 1489–1511.

Iervolino I, Spillatura A, Bazzurro P. (2018). Seismic Reliability of Code-Conforming Italian Buildings. Journal of Earthquake Engineering, 22:sup2, 5-27, DOI: 10.1080/13632469.2018.1540372

Iervolino, I., Baraschino, R., Spillatura, A. (2021). Evolution of seismic reliability of code-conforming Italian buildings. Submitted to Journal of Earthquake Engineering.

Kremmyda, G. D., Fahjan, Y. M., and Tsoukantas, S. G. (2014). Nonlinear FE analysis of precast RC pinned beam-to-column connections under monotonic and cyclic shear loading. Bull. Earthqu. Eng. 12, 1615–1638. doi:10.7712/ 120113.4611.c1443

Kremmyda, G. D., Fahjan, Y. M., Psycharis, I. N., and Tsoukantas, S. G. (2017). Numerical investigation of the resistance of precast RC pinned beam-to- column connections under shear loading. Earthqu. Engng Struct. Dyn. 46 (9), 1511–1529. doi:10.1002/eqe.2868

Legge 25 novembre 1962, n. 1684. Provvedimenti per l'edilizia, con particolari prescrizioni per le zone sismiche (Gazzetta Ufficiale 22 dicembre 1684, n. 326). (in Italian)

Liberatore L, Noto F, Mollaioli F, Franchin P. (2018). 'In-plane response of masonry infill walls: Comprehensive experimentally-based equivalent strut model for deterministic and probabilistic analysis', Engineering Structures 167: 533–548

Magliulo G, Bellotti D, Cimmino M, Nascimbene R. (2018). Modeling and Seismic Response Analysis of RC Precast Italian Code-Conforming Buildings. Journal of Earthquake Engineering, 22:sup2, 140-167, DOI: 10.1080/13632469.2018.1531093

Magliulo G, Di Salvatore C, Ercolino M. (2021). Modeling of the Beam-To-Column Dowel Connection for a Single-Story RC Precast Building. Front. Built Environ. 7: 627546. Doi: 10.3389/fbuil.2021.627546

Magliulo G, Ercolino M, Cimmino M, Capozzi V, Manfredi G. (2014). FEM analysis of the strength of RC beam-to-column dowel connections under monotonic actions. Construct Build Mater. 69:271-284

Magliulo, G., Capozzi, V., Fabbrocino, G., and Manfredi, G. (2011). "Neoprene-concrete friction relationships for seismic assessment of existing precast buildings." Eng Struct, 33(2), 532-538

Magliulo, G., Ercolino, M., Petrone, C., Coppola, O., Manfredi, G. (2014). The Emilia earthquake: seismic performance of precast reinforced concrete buildings. Earthquake Spectra, 30(2):891–912. doi: 10.1193/091012EQS285M.

Mander J. B., Priestley M. J. N., Park R. (1988). Theoretical Stress-Strain Model for Confined Concrete. ASCE Journal of Structural Engineering, 114 (8):1804-1826.

Menichini, G., Del Monte, E., Orlando, M., and Vignoli, A. (2020). Out-of-plane capacity of cladding panel-to-structure connections in one-story R/C precast structures. Bulletin of Earthquake Engineering, 18:6849–6882.

Metelli G, Beschi C, Riva P. (2011). Cyclic behaviour of a column to foundation joint for concrete precast structures. Eur J Environ Civ Eng. 15(9):1297-1318

Metelli, G., Riva, P. (2007). Behaviour of a support system for precast concrete panels. Proceedings of the 6th International Conference on Fracture Mechanics of Concrete and Concrete Structures, 2: 951–61.

Minghini, F., Ongaretto E., Ligabue V., Savoia M., Tullini N. (2016). Observational failure analysis of precast buildings after the 2012 Emilia earthquakes. Earthquakes and Structures 11(2): 327–46. doi:10.12989/eas.2016.11.2.327.

Nastri, E., Vergato M., Latour, M. (2017). Performance evaluation of a seismic retrofitted R.C. precast industrial building. Earthquakes and Structures 12(1). doi: 10.12989/eas.2017.12.1.013.

Osanai Y, Watanabe F, Okamoto S. (1996). Stress transfer mechanism of socket base connections with precast concrete columns. ACI Struct J. 93(3):266-276.

Palanci, M., Senel, S. M., and Kalkan, A. (2017). Assessment of one story existing precast industrial buildings in Turkey based on fragility curves. Bull. Earthq. Eng. 15 (1), 271–289. doi:10.1007/s10518-016-9956-x

Regio Decreto 16 novembre 1939-XVIII, n. 2229. Norme per la esecuzione delle opere in conglomerato cementizio semplice od armato. (in Italian)

Rodrigues H, Vitorino H, Batalha N, Sousa R, Fernandes P, Varum H. (2021). Influence of Beam-to-Column Connections in the Seismic Performance of Precast Concrete Industrial Facilities. Structural Engineering International, DOI: 10.1080/10168664.2021.1920082

Savoia M., Mazzotti C., Buratti N., Ferracuti B., Bovo M., Ligabue V. (2012). Damages and collapses in industrial precast buildings after the Emilia earthquake. Ingegne. Sismi. 29, 120–131

Scotta R., De Stefani L., Vitaliani R. (2015). Passive control of precast building response using cladding panels as dissipative shear walls. Bull. Earthqu. Eng. 13, 3527–3552. doi:10.1007/s10518-015-9763-9

Sousa R, Batalha N, Rodrigues H. (2020a). Numerical simulation of beam-to-column connections in precast reinforced concrete buildings using fibre-based frame models. Engineering Structures, 203:109845.

Sousa R, Batalha N, Silva V, Rodrigues H. (2020b). Seismic fragility functions for Portuguese RC precast buildings. Bull Earthquake Eng. https://doi.org/10.1007/s10518-020-01007-7

Toniolo G., Colombo A. (2012). Precast concrete structures: the lessons learned from the L'Aquila earthquake. Structural Concrete, 13(2):73-83

1   Torquati, M., Belleri, A., Riva, P. (2018). Displacement-Based Seismic Assessment for Precast
2   Concrete Frames with Non-Emulative Connections. Journal of Earthquake Engineering. doi:
3   10.1080/13632469.2018.1475311.

4   Verderame G. M., Ricci P., Esposito M., Sansiviero F. C., 'Le caratteristiche meccaniche degli acciai
5   impiegati nelle strutture in c.a. realizzate dal 1950 al 1980', Atti del XXVI Convegno Nazionale
6   AICAP "Le prospettive di sviluppo delle opere in calcestruzzo strutturale nel terzo millennio",
7   Padova, 19-21 maggio 2011. (in Italian)

8   Verderame G.M., Ricci P. (2018). An empirical approach for nonlinear modelling and deformation
9   capacity assessment of RC columns with plain bars. Engineering Structures, 176, 539-554.

10   Zoubek, B., Fahjan, Y., Fischinger, M., and Isakovic, T. (2014). Nonlinear finite element modelling
11   of centric dowel connections in precast buildings. Eng. structures 14 (4), 463–477.
12   doi:10.12989/cac.2014.14.4.463

13   Zoubek, B., Fischinger, M., and Isakovic, T. (2015). Estimation of the cyclic capacity of beam-to-
14   column dowel connections in precast industrial buildings. Bull. Earthqu. Eng.13 (7), 2145–2168.
15   doi:10.1007/s10518-014- 9711-0

16   Zoubek, B., M. Fischinger, and T. Isaković. (2016). Cyclic response of hammer-head strap cladding-
17   to-structure connections used in RC precast building. Engineering Structures 119: 135–48.